Hairpin-Forming Peptide Nucleic Acid Oligomers†

Bruce Armitage,‡,§ Danith Ly,§ Troels Koch,|| Henrik Frydenlund,|| Henrik Ørum,|| and Gary B. Schuster*,§

School of Chemistry and Biochemistry, Georgia Institute of Technology, Atlanta, Georgia 30332-0400, and PNA Diagnostics A/S, Rønnegade 2, DK-2100 Copenhagen, Denmark

Received December 2, 1997; Revised Manuscript Received May 7, 1998

ABSTRACT: A series of partially self-complementary peptide nucleic acid (PNA) oligomers was prepared. Examination of their melting behavior, circular dichroism spectra, and fluorescence properties reveals that these PNA oligomers exist as stem-loop ("hairpin") structures. Fluorescence is readily observed in hairpins containing a covalently linked, emissive acridine derivative which is, at least partially, intercalated in the duplex region of the PNA hairpin. The acridine fluorescence is quenched when an anthraquinone derivative is covalently attached to the PNA so that it is bound near the acridine in the hairpin structure. Acridine fluorescence is restored in hairpins containing both the anthraquinone and the acridine by increasing the temperature and melting the structure to its linear form or by opening the hairpin through formation of a hybrid duplex with complementary DNA. The latter process may form the basis for development of selective and sensitive DNA assays.

Over the past decade, there has been considerable interest in the development of synthetic structures that specifically recognize and bind selectively to DNA and RNA sequences for use as diagnostic or therapeutic agents (*1*). Peptide nucleic acid (PNA) oligomers are unrivaled in their successful accomplishment of this goal (*2*). PNA is an analogue of DNA and RNA in which the natural scaffold of sugars linked by phosphates is replaced by (2-aminoethyl)glycine units linked to nucleobases by acyl groups (see Chart 1) (*3*−*5*).

Remarkably, PNA oligomers form duplex and higher-order structures that follow the Watson−Crick and Hoogsteen base-pairing rules. When the PNA oligomer contains both purine and pyrimidine nucleobases, it will hybridize with complementary PNA, DNA, or RNA to form a right-handed double-helical duplex (*6*−*8*). The mixed-sequence hybrid PNA/DNA and PNA/RNA duplexes and the $(PNA)_2$ duplexes have greater stability than their all natural $(DNA)_2$ and $(RNA)_2$ homologous structures (*9*). Homopyrimidine PNA strands react with complementary single-stranded DNA to form $(PNA)_2$/DNA triplexes (*3*−*5*). With duplex DNA, homopyrimidine PNA reacts to form strand-invasion complexes where the noncomplementary strand separates as a single-stranded D-loop: $(PNA)_2$/DNA−DNA (*10*−*12*). Covalent attachment of the two homopyrimidine PNA strands by a flexible linker stabilizes the strand-invasion complex significantly (*13*). It was reported recently that three PNA strands self-associate to form PNA triplexes (*14*). Clearly, PNA oligomers are able to adopt structures that mimic those of natural DNA and RNA oligonucleotides.

Chart 1

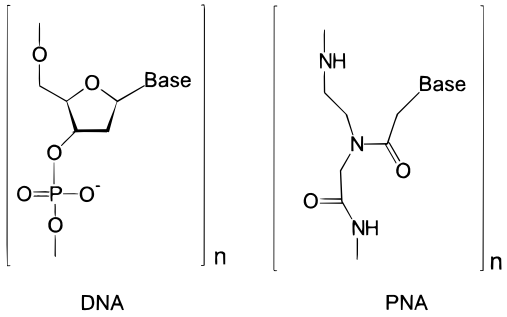

Single-stranded DNA and RNA oligomers having self-complementary sequences will form stem-loop-containing structures known as "hairpins" (*15*). These structures offer a special opportunity to control the distance between portions of the DNA or RNA. In the hairpin form, groups on or near complementary bases in the duplex region are close together. When the hairpin is opened to its linear form, groups that were close together can become far apart. Tyagi and Kramer recently reported a clever application of this phenomenon in the development of nucleic acid probes, useful in diagnoses, that they characterize as "*Molecular Beacons*" (*16*).

Assays for nucleic acids can be considered to be heterogeneous or homogeneous. In a heterogeneous assay the probe typically is bound to a solid surface and its association with the targeted nucleic acid elicits a measurable response. Wang and co-workers recently reported the first use of PNA oligomers as the recognition element in a heterogeneous DNA biosensor operating by electrochemical detection of the hybridization event (*17, 18*). PNA was found to offer special advantages in this assay. Homogeneous nucleic acid assays in solution generally rely on the spatial dependence of interaction between groups on the probe and target strands to signal hybridization. In the *Molecular Beacons*, for example, hybridization changes the distance between a fluorescer linked covalently to the 5′-terminus of a hairpin-forming

† This work was supported by funding from the National Institutes of Health (Grant PHS NRSA GM16498-01 to B.A. and Grant RO1 GM28190 to G.B.S.).

‡ Current address: Department of Chemistry, Carnegie Mellon University, Pittsburgh, PA 15213.

§ Georgia Institute of Technology.

|| PNA Diagnostics A/S.

S0006-2960(97)02945-0 CCC: $15.00
Published on Web 06/11/1998

Scheme 1. Synthesis of PNA−Anthraquinone Linked Monomer (Q)

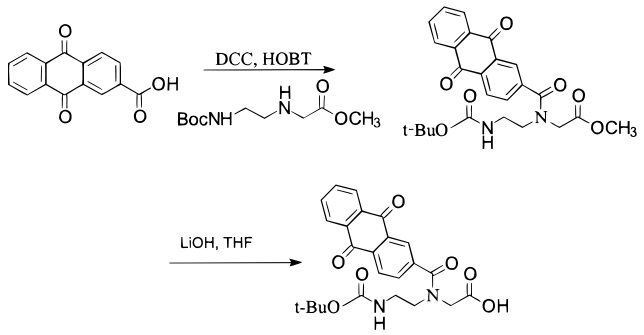

Monomer Q

DNA oligomer and a quencher linked to its 3′-terminus. In the hairpin form, the fluorescer and quencher are close and energy transfer reduces the fluorescence intensity. Hybridization of the probe with a complementary target DNA converts the hairpin to its linear form, increasing the distance between the fluorescer and quencher, thus reducing the quenching rate and causing a measurable increase in fluorescence efficiency.

We report herein the preparation and analysis of partially self-complementary PNA oligomers. Their physical and spectroscopic properties show that they exist as hairpin structures in solution. PNA offers the advantage of easy incorporation of nonnucleobase substituents at internal positions and the unique ability to form stable duplexes at low salt concentration. We incorporated a fluorescer and an electron-transfer quencher into the duplex region of the hairpin PNA. Reaction of the hairpin PNA with a complementary DNA oligomer yields a linear PNA/DNA hybrid duplex with unique spectral properties. This process provides the basis for development of homogeneous nucleic acid assays.

RESULTS

(1) Synthesis of PNA−Aminoacridine−Anthraquinone Conjugates. Protected PNA monomers having an anthraquinone or aminoacridine group linked covalently to the "backbone" nitrogen atom of the (2-aminoethyl)glycine were prepared by the methods outlined in Schemes1 and 2, respectively. The details of these syntheses and the characterization of the monomers are described in the Experimental Section. Three PNA oligomers (see Scheme 3) were synthesized from *N*-Boc-protected (2-aminoethyl)glycine monomers by solid-state methods. The primary structures of the oligomers were confirmed by MALDI-TOF mass spectrometry.

PNA(1) is a 23-mer with two lysines added to the C-terminus for solubility. This PNA oligomer was designed so that it contains a series of nine self-complementary bases at each end separated by a five-base sequence. DNA sequences having related primary structures exist in solution as a hairpin where the self-complementary segments form a duplex stem that is bridged by a single-stranded loop. Hairpin structures have not been previously characterized in PNA oligomers. In PNA(2), the adenine at position 6 in PNA(1) is replaced in the synthesis by the acridine-containing monomer (Ar). In PNA(3), the adenine at position 19 of PNA(1) is replaced by the quinone-containing monomer (Q) and the adenine at position 6 is replaced by Ar. The base opposite Ar and Q is thymine in all cases, selected to provide the most space for intercalation of the substituent.

(2) Characterization of PNA−Aminoacridine-Anthraquinone Conjugates and Hybrid Duplexes. (a) Melting Behavior. Nucleic acid oligomers containing self-complementary sequences may form intramolecular hairpin structures, or they can aggregate to form bimolecular (or higher) structures (*19*). A typical example of a potential hairpin-forming structure is DNA(1) (Scheme 3). It has a nine-base-pair self-complementary sequence extending from the 3′-terminus and the 5′-terminus that is separated by a five-base noncomplementary sequence. The melting behavior of an oligomer can be used to distinguish hairpin structures from aggregates. Hairpins generally show a concentration-independent melting temperature (T_m), whereas the T_m for aggregated structures is typically concentration-dependent. The melting behavior of DNA(1) was determined by UV spectroscopy in phosphate-buffered solution. It shows a single transition at 45 °C over a concentration range from 0.4 to 5.0 μM. Absorption and first-derivative plots for the melting of DNA(1) are shown in Figure 1. These findings are characteristic of hairpin-forming DNA oligomers (*20*). The base sequence in PNA(1) is identical with that of DNA(1), with the 5′-terminus of the DNA corresponding to the C-terminus of the PNA. We anticipated that PNA(1) might also exist primarily in the hairpin form.

The melting behavior of PNA(1) was examined to probe its structure. Samples of PNA(1) in 10 mM sodium phosphate buffer solution (pH = 7.0) were heated to 90 °C for 5 min to ensure denaturation and then cooled slowly to room temperature to permit hybridization. The T_m of the structure formed was measured by monitoring its absorption intensity at 260 nm as the temperature of the sample was increased from 20 to 90 °C at 0.5 °C/min. The absorbance change and first-derivative plots (see Figure 1) obtained for PNA(1) reveal a single transition with T_m = 81 °C. The T_m of PNA(1) is independent of concentration from 0.4 to 7.5 μM (data not shown). This result suggests that, like its DNA analogue, PNA(1) forms an intramolecular hairpin structure. Typical of PNA oligomers, the T_m of PNA(1) is considerably higher than that of DNA(1) (*21*).

The melting behavior of PNA(2) and PNA(3) was also investigated. These structures have nonbase-pairing substituents (an acridine, and both a quinone and an acridine, respectively) in place of adenines. This substitution will cause T_m to decrease because of the loss of hydrogen bond stabilization. The temperature dependence of the absorption for PNA(2) and PNA(3) is complex (Figure 2). In particular, they both show melting transitions at about 60 °C, but especially for PNA(3), several additional transitions are apparent indicating that a mixture of structural forms exists.

PNA and DNA form hybrid duplex structures according to the Watson−Crick base-pairing rules. When equimolar amounts of PNA(1) and DNA(1) are hybridized in phosphate buffer solution, the melting transition characteristic of DNA(1) in its hairpin form is absent. In its place is a single transition with T_m = 82 °C (Figure 1). This finding supports formation of a PNA/DNA hybrid duplex that is more stable than its DNA hairpin precursor. PNA(2) and PNA(3) also form hybrid duplexes with DNA(1). The melting behavior of these duplexes is shown in Figure 3. For both cases, a $T_m \approx 76$ °C is observed. We recently showed that a hybrid

Scheme 2. Synthesis of PNA−Aminoacridine Linked Monomer (Ac)

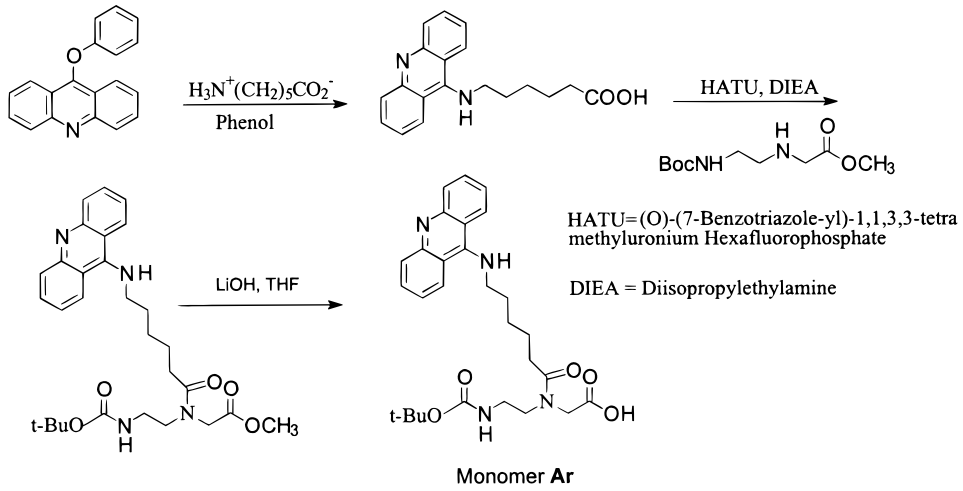

Scheme 3. Nucleic Acid Oligomers in Hairpin Form

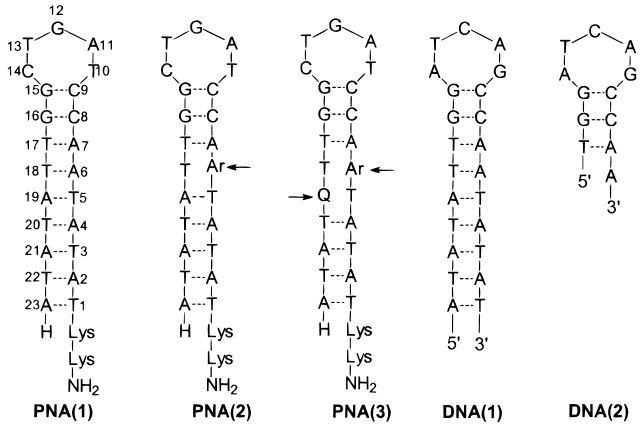

duplex formed by DNA and a PNA−anthraquinone conjugate was stabilized by intercalation of the quinone which resulted in an increased T_m (*22*).

(b) Circular Dichroism Spectroscopy. Buchardt and co-workers (*23*) showed that hybrid PNA/DNA and PNA/RNA duplexes exhibit observable circular dichroism (CD) spectra. More recently, Nielsen, Nordén, and co-workers (*24*−*26*) showed that $(PNA)_2$ duplexes exhibit CD spectra induced by a chiral amino acid at the C-terminus and propagated by induction of helicity through the achiral backbone of the PNA oligomer. We examined the CD spectrum of PNA(1) to probe its structure.

The CD spectrum of a 2.5 μM solution of PNA(1) in phosphate buffer at 20 °C is shown in Figure 4. It is typical of the CD spectra reported by Nielsen and Nordén for duplex PNA. When the solution is heated to 90 °C, a temperature above T_m for PNA(1), the CD spectrum disappears (data not shown). These results are consistent with a hairpin structure for PNA(1).

The CD spectrum of DNA(1), Figure 4, is typical of duplex DNA. Significantly, the CD spectrum of the structure formed from a 1:1 mixture of PNA(1) and DNA(1), shown also in Figure 4, is not the sum of its components. Indeed, the spectrum of the PNA(1)/DNA(1) hybrid duplex is stronger than either parent and its maximum is shifted. When the solution of the hybrid duplex is heated to 95 °C, above its T_m, the CD spectrum observed is identical with that of single-stranded DNA(1) at this temperature. Importantly, formation of a PNA/DNA hybrid duplex from PNA(1) does not require a full complementary DNA sequence. The hybrid formed from DNA(2), complementary only to the loop and a portion of the stem, and PNA(1) gives a CD spectrum nearly identical to that observed from the PNA(1)/DNA(1) duplex (data not shown). Clearly, the DNA(2) dodecamer is capable of opening the hairpin of PNA(1) and forming a partial hybrid duplex. At 85 °C, where the hybrid duplex has melted, the CD spectrum of PNA(1)/DNA(2) is identical to that of single-stranded DNA(2). The CD spectra of PNA-(2), which has a conjugated aminoacridine in place of a base, and of PNA(3), which has both acridine and anthraquinone substituents, are both essentially identical with that of PNA-(1). This suggests that these two compounds exist as hairpins with structures similar to that of PNA(1). Significantly, when DNA(2) is mixed with PNA(2) or PNA(3) the resulting CD spectra become virtually identical with those seen for the PNA(1)/DNA(1) and PNA(1)/DNA(2) hybrid duplexes.

(3) Fluorescence of PNA−Aminoacridine−Anthraquinone Conjugates and Hybrid Duplexes. The findings described above suggest that these PNA hairpins recognize complementary single-stranded DNA and form a hybrid duplex structure. Critically, this hybridization will change the distance between substituents on the PNA backbone located in its stem region. Complementary bases that were linked by Watson−Crick hydrogen bonding in the hairpin may be separated by many bases in the hybrid duplex. We tested this predicted change by utilizing the fluorescence of aminoacridine as an indicator of hybrid duplex formation.

In its hairpin form, the anthraquinone and acridine substitiuents of PNA(3) are in direct contact on adjacent positions in the stem region (see Scheme 3). Figure 5 shows the effect of heating a phosphate-buffered solution of PNA-(3) on the fluorescence of the aminoacridine group. The fluorescence intensity (λ_{exc} = 417 nm, only the acridine absorbs) changes very little as the temperature is increased from 25 to 45 °C, but it increases dramatically as the temperature is raised beyond 50 °C. This behavior mimics the melting behavior of PNA(3) and reflects its transition from a hairpin structure to the single-stranded form. As a control experiment, we examined the temperature dependence of the aminoacridine fluorescence for PNA(2) which does not have an anthraquinone substituent. Unlike PNA(3), there is a slight decrease in the fluorescence intensity between the

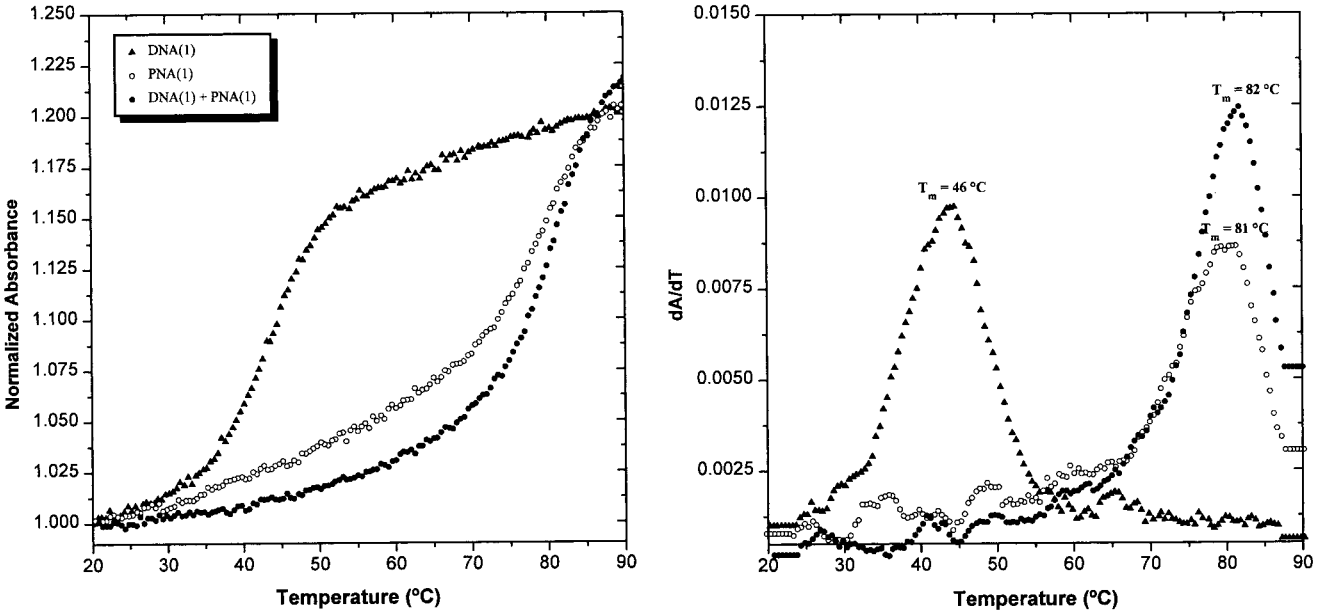

FIGURE 1: Change in absorption (left) and first-order derivative melting curves (right) for heating runs monitored at 260 nm in 10 mM $NaPO_4$ buffer solution at pH 7.0. The concentration of single-strand or duplex structures in each sample is 2.5 μM: DNA(1), T_m = 45 °C, hairpin; PNA(1), T_m = 81 °C, hairpin; DNA(1) + PNA(1), T_m = 82 °C, linear duplex.

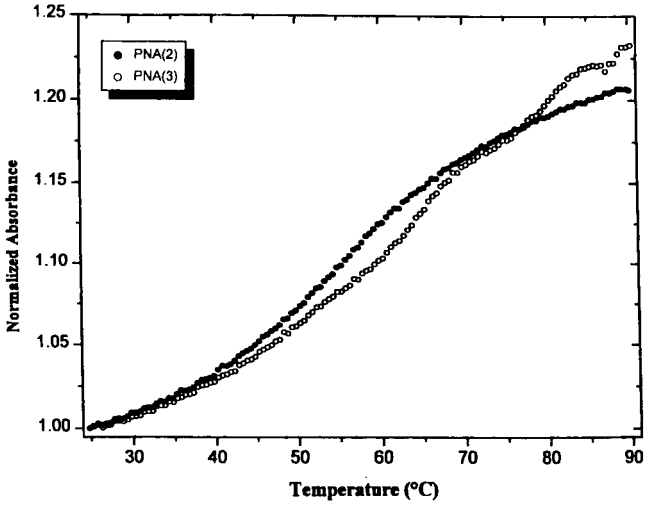

FIGURE 2: Change in absorbance (normalized to the initial absorption intensity) on heating of PNA(2) and PNA(3). The concentration of oligomer in each sample is 2.5 μM in 10 mM $NaPO_4$ buffer solution at pH 7.0: PNA(2), $T_m \approx 60$ °C, hairpin PNA(3), $T_m \approx 60$ °C, hairpin: multiple transitions.

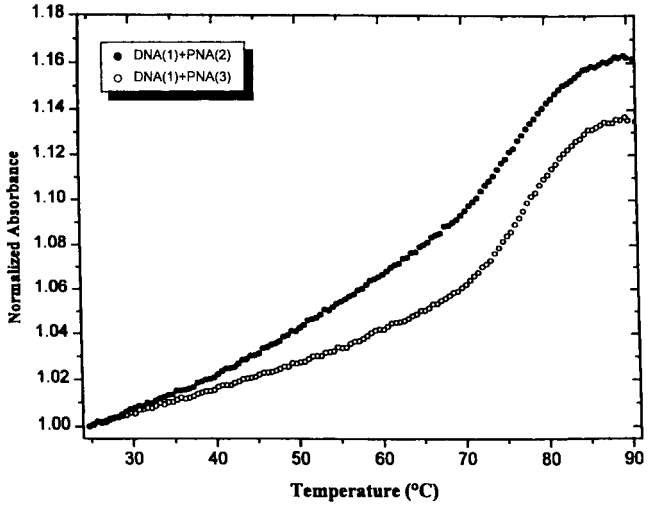

FIGURE 3: Change in absorbance on heating of the PNA/DNA hybrid duplex. The concentration of duplex in each sample is 2.5 μM in 10 mM $NaPO_4$ buffer solution at pH 7.0: DNA(1) + PNA-(2), $T_m \approx 76$ °C, linear duplex; DNA(1) + PNA(3), $T_m \approx 76$ °C, linear duplex.

hairpin and single-stranded forms of PNA(2). Clearly, the adjacent anthraquinone group quenches the aminoacridine fluorescence in the hairpin form of PNA(3), and this quenching is reduced or eliminated when these two groups are separated by 12 bases in the single-stranded form.

Formation of a hybrid duplex between PNA(3) and DNA-(1) will also open the hairpin structure of the PNA and separate the quinone and acridine by 12 base pairs placing each opposite a thymidine on the DNA strand (Scheme 4). Figure 6 shows a "titration plot" of fluorescence intensity recorded as the amount of DNA(1) added to a solution of PNA(3) is increased. The intensity rises monotonically until the ratio of PNA to DNA is 1:1, and then it remains constant as more DNA is added. This is clear evidence that formation of the hybrid duplex is accompanied by an increase in the aminoacridine fluorescence efficiency. The titration of PNA-(2), which has the acridine substituent but not the quinone, with DNA(1) is also shown in Figure 6. In this case the fluorescence intensity in the absence of complementary DNA(1) is high and hybridization causes only a small increase in intensity. In the presence of excess DNA(1), the fluorescence from PNA(3)/DNA(1) and from PNA(2)/DNA-(1) hybrid duplexes is essentially identical.

DNA(1) evidently forms a 1:1 hybrid duplex with PNA-(3) that opens the hairpin structure of both oligonucleotides causing an increase in the aminoacridine fluorescence efficiency. We have shown that anthraquinone substituents intercalate in PNA/DNA hybrid duplexes (*22*), and we expect that the acridine substituent is associated similarly since it does intercalate in DNA (*27*). The major effect of hybrid duplex formation on the aminoacridine fluorescence in PNA-(3)/DNA(1) is the increased distance to the quinone, not the

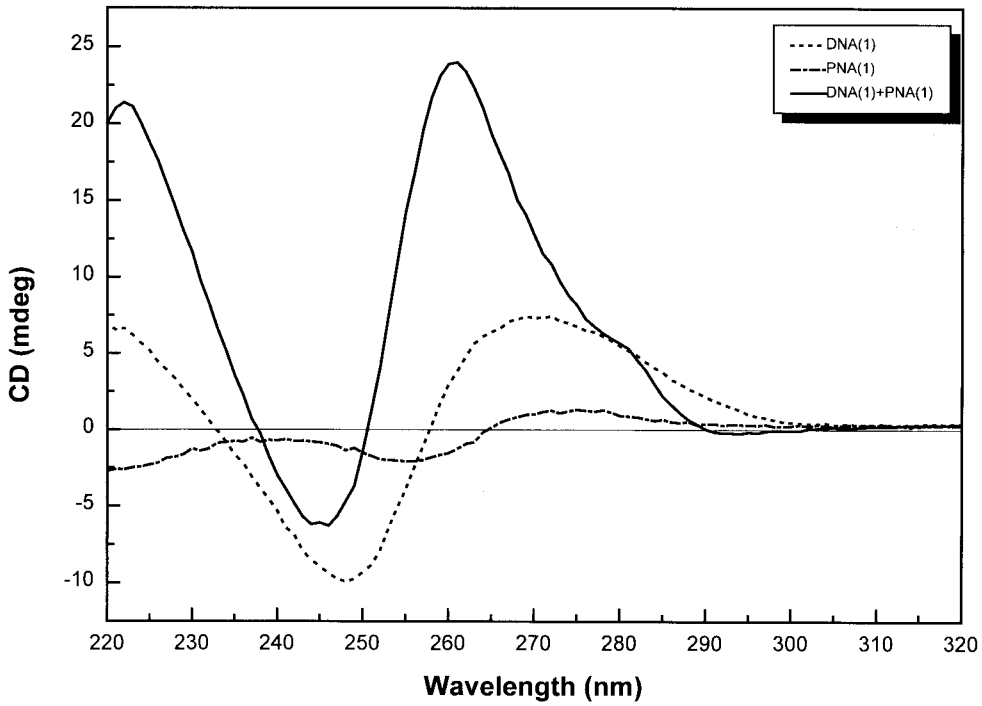

FIGURE 4: CD spectra (220−320 nm) of DNA(1) and PNA(1) recorded at 20 °C. The concentration of oligomers or duplex structures in each sample is 2.5 μM in 10 mM $NaPO_4$ buffer solution at pH 7.0: DNA(1), hairpin; PNA(1), hairpin; DNA(1) + PNA(1), linear duplex.

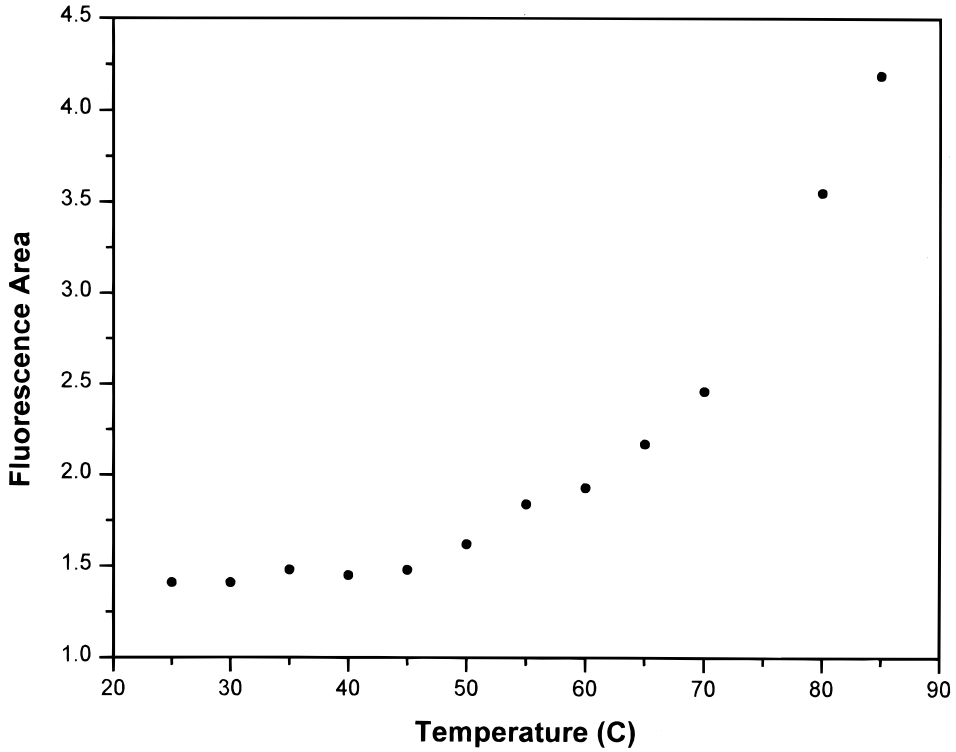

FIGURE 5: Fluorescence intensity (excited at 417 nm, emission integrated from 430 to 600 nm) of PNA(3) as a function of temperature in 10 mM $NaPO_4$ buffer solution at pH 7.0. The concentration of the PNA oligomer is 2.5 μM. The fluorescence area is in arbitrary units.

intercalation of the acridine group in the hybrid duplex. The latter effect is responsible for the increase in aminoacridine fluorescence in the PNA(2)/DNA(1). As a further control, we examined the effect of adding a 5-fold excess of noncomplemetary single-stranded DNA to PNA(3). The added DNA causes no measurable effect on the aminoacridine fluorescence intensity, and it does not interfere with the fluorescence enhancement caused by DNA(1). The intensity increase must be a consequence of selective association of PNA(3) and DNA(1), and not an effect of nonspecific binding.

The hairpin structure of PNA(3) is opened by DNA oligomers complementary to only a portion of its sequence. Addition of DNA(2) to a solution of PNA(3) results in an increase in aminoacridine fluorescence that parallels the effect of added DNA(1) (Figure 7). However, the fluorescence enhancement with DNA(2) is less than that caused by DNA(1). Evidently, the unhybridized, single-stranded portion of

Scheme 4. PNA/DNA Hybrid Formation

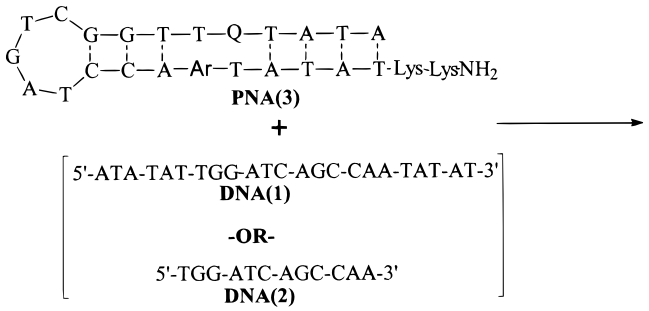

PNA(3): H_2N-Lys-Lys-TAT-ATAr-ACC-TAG-TCG-GTT-QTA-TA
DNA(1): 5'-ATA-TA T- TGG-ATC-AGC-CAA-TAT-AT-3'

-OR-

PNA(3): H_2N-Lys-Lys-TAT-ATAr-ACC-TAG-TCG-GTT-QTA-TA
DNA(2): 5'-TGG-ATC-AGC-CAA-3'

the PNA(3)/DNA(2) allows quenching of the acridine excited state that is inhibited when the fluorescer is incorporated in the duplex part of the structure.

DISCUSSION

(1) Hairpin PNA. Stem-loop (hairpin) RNA and DNA structures are known to form readily from appropriate nucleic acid sequences (*15*). Given the uncanny ability of PNA to imitate the Watson−Crick base-pairing properties of the natural nucleic acids, there seemed to be little doubt that these nucleic acid mimics would also form hairpin structures. PNA(1) is the first example we are aware of that verifies this prediction. The melting and spectroscopic behavior observed for this compound shows that it adopts the hairpin structure depicted in Scheme 3. Characteristically, the thermodynamic stability of the PNA(1) structure, revealed by its melting temperature, is greater than that observed for DNA(1) which contains an identical sequence. This increase in stability offers potential advantages in the use of PNA derivatives as biosensors (*17*, *18*). In particular, for cases where a change in spatial relationship provides the detected signal, PNA may provide spatial differentiation with fewer bases than the comparable DNA-based sequence. Exploitation of this advantage requires the ability to prepare specific PNA sequences covalently linked to "reporter" units that do not completely disrupt the hairpin structure. We have developed synthetic technology to incorporate reporter groups linked to internal PNA positions.

PNA(2) contains an aminoacridine group in place of one of the nucleic acids on the PNA backbone. By design, the acridine group falls within the duplex region of the PNA hairpin. The melting behavior and, especially, circular dichroism spectroscopy indicate that incorporation of the acridine does not prohibit hairpin formation. Similarly, the evidence indicates that PNA(3), which contains two non-nucleic acid groups (an acridine and an anthraquinone) bound in the duplex region of the hairpin, also maintains the ability to form stem-loop structures. The melting behavior of PNA(2) and PNA(3) is not as simply interpreted as for PNA(1) since several transitions are observed. However, on the basis of the CD spectroscopy, there is little doubt that the gross structures of these three compounds are similar. The complex melting behavior of PNA(2) and PNA(3) may indicate local disorder of the structure near the attachment sites of the reporter groups. Additional work is under way to assess this issue in greater detail.

(2) Recognition of DNA. A nucleic acid probe must recognize its complement selectively and initiate a unique, sensible event. The unrivaled ability of PNA to form duplex, and higher-order, structures with complementary DNA and RNA suggested that its modification to include reporter groups would not destroy the recognition ability. The experiments described above reveal this to be the case. The melting behavior observed for mixtures of PNA(1) and DNA(1), its full-length complement, confirms the formation of a hybrid structure. Analysis of the CD spectrum of this structure supports formation of the expected linear duplex.

The use of PNA hairpin structures as sequence-specific DNA probes will generally require recognition of DNA that is not complementary to the entire PNA sequence. Hairpin formation, required for the spatial manipulation of the reporter groups, necessitates partially self-complementary structures for the PNA that will not be found generally in the targeted DNA. This critical ability of PNA(1) was demonstrated by its reaction with DNA(2): a dodecamer complementary to only the loop and a portion of the stem region of the PNA. The melting behavior and the CD spectroscopy of the PNA(1)/DNA(2) structure indicate formation of a hybrid structure that has opened the PNA hairpin. This conclusion is supported further by the fluorescence behavior of PNA(3) in the presence of DNA(1) and DNA(2).

(3) Aminoacridine Fluorescence Quenching: A Probe of Structure and Electron (Hole) Transport in PNA/DNA Hybrids. The difference in fluorescence intensity between the hairpin form of PNA(3) and its hybrid duplex with DNA(1) will be controlled both by structure and by the photophysics of acridine quenching. The aminoacridine unit of nonnucleotide substituent Ar is linked to the PNA backbone through a carbon−nitrogen bond to its 9-amino group. While the properties of 9-aminoacridine have been extensively studied, there are only a few reports concerning the mono N-alkylated aminoacridines. We use 9-(*N*-methylamino)-acridine as a model for the acridine group of Ar. In acetonitrile solution, the fluorescence quantum yield (Φ_{fl}) for 9-aminoacridine is 0.96 and its singlet lifetime is 15.8 ns (*28*). In contrast, under these conditions the Φ_{fl} for 9-(*N*-methylamino)acridine is only 0.011 and its singlet lifetime is correspondingly reduced to 2 ns. This dramatic change in photophysical properties caused by methyl substitution is mirrored in a comparison of photoelectron spectra (*29*). These effects are attributed to a change in excited-state character caused by loss of overlap of the acridine π-electron system with the nonbonding electrons of the amino nitrogen atom due to steric effects when the methyl group of 9-(*N*-methylamino) derivative is coplanar with the acridine. The reduced lifetime of the methylaminoacridine makes it less susceptible to fluorescence quenching by guanine and adenine (*28*). Consequently, we observe little difference in the aminoacridine fluorescence intensity between the hairpin and linear forms of PNA(2).

The aminoacridine fluorescence of PNA(3) is quenched when it is in its hairpin form. We attribute this to electron transfer from the excited singlet state of the acridine to the

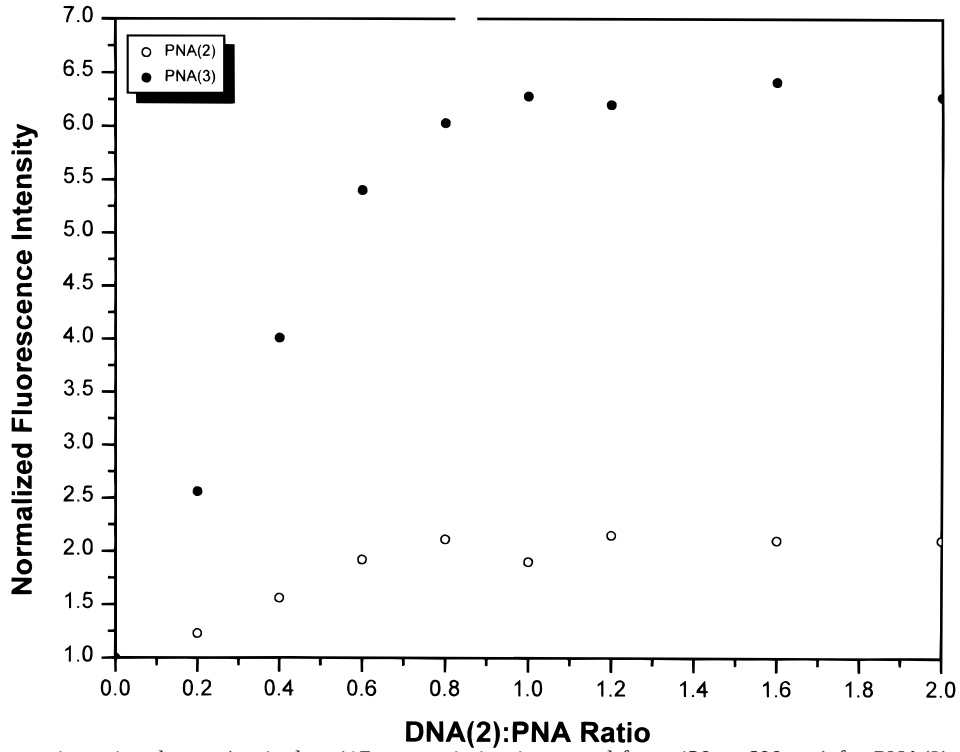

FIGURE 6: Fluorescence intensity change (excited at 417 nm, emission integrated from 430 to 600 nm) for PNA(2) and PNA(3) titrated with DNA(2) in 10 mM $NaPO_4$ buffer solution at pH 7.0. The concentration of each of the PNA oligomers is 0.5 μM. The fluorescence intensity is normalized to that of the PNA sample with no DNA present.

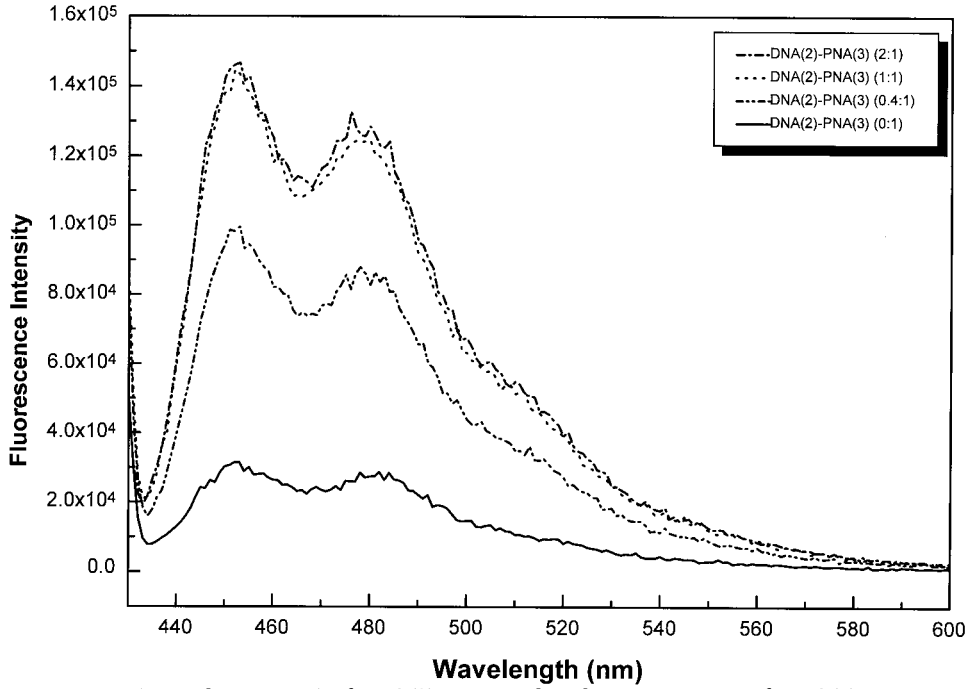

FIGURE 7: Fluorescence spectra (excited at 417 nm) of PNA(3) monitored as the concentration of DNA(2) is increased from 0 to 1.0 μM in 10 mM $NaPO_4$ buffer solution at pH 7.0. The PNA(3) concentration is 0.5 μM in all samples. The fluorescence intensity is in arbitrary units.

nearby anthraquinone group. The oxidation potential of 9-(*N*-methylamino)acridine is reported to be 0.21 V versus SCE (*30*). The reduction potential of anthraquinone derivatives closely related to Q is −0.58 V versus SCE (*31*). The energy of the singlet excited state of the aminoacridine in PNA(2) calculated from its fluorescence spectrum is 2.82 eV. Application of the Weller equation (*32*) ignoring the Coulomb work term, which should be negligible, reveals that the free energy for electron transfer (ΔG_{et}) is −2.03 eV for transfer of an electron from the singlet excited state of the aminoacridine to the anthraquinone. This reaction is sufficiently exothermic for it to occur at essentially every encounter between the excited acridine and the quinone.

Despite this result, there is weak residual aminoacridine fluorescence from the hairpin form of PNA(3). We attribute this to multiple conformations of the quinone and acridine groups as is suggested by its multiphase melting behavior. If the excited-state aminoacridine group is in contact with

the quinone, then quenching should be nearly instantaneous and complete. The precise meaning of "contact" is not clearly defined by these experiments. We take it, provisionally, to mean that both the quinone and acridine are intercalated within the duplex region of the PNA hairpin. In this regard, if either the quinone or the acridine is extrahelical when the acridine is excited, it seems unlikely that binding within the duplex will occur within the ~2 ns lifetime of the excited state. The data in Figure 5 show that the aminoacridine fluorescence increases about 3.3-fold when PNA(3) is converted from its hairpin to its linear form. Interpreted within the multiconformational model, this finding indicates that the ratio of PNA(3) structures where quinone/acridine is in contact to those where one group is extrahelical is about 3.3:1.

The data in Figure 6 show that the reaction of PNA(3) with DNA(1) results in a ~6.5-fold increase in aminoacridine fluorescence intensity. We attribute this to conversion of the hairpin form of the PNA to a linear hybrid duplex in which the acridine and quinone are no longer in contact. There has been considerable recent discussion concerning the ability of DNA to conduct holes (radical cations) and electrons (*33*). Barton and co-workers (*34*−*36*) have argued for very rapid transport. Meade and co-workers (*37*) report a slower rate. Our findings suggest that, on the short time scale of the aminoacridine lifetime, the PNA/DNA hybrid duplex behaves more like an insulator than a conductor (*22*). Thus, whether intercalated or not, the quinone does not efficiently quench the aminoacridine fluorescence when the two groups are separated by twelve base pairs in the hybrid duplex.

(4) Application of PNA Hairpin Structures as Nucleic Acid Probes. The use of PNA in the construction of probes to sense nucleic acids may offer several advantages over using DNA as the sequence-selective recognition element. PNA/DNA hybrid duplexes provide exquisite single-base mismatch selectivity (*18*) and offer greater stability than their DNA/DNA or DNA/RNA counterparts, especially in solutions with low salt concentration. This may be particulaly helpful in the hairpin format of the *Molecular Beacons*. The duplex region of the hairpin will generally not be fully complementary to the targeted nucleic acid, and this region can be shorter for a PNA probe than for a DNA probe. Also, since PNA is unnatural, there are no nuclease or protease enzymes that destroy it. This offers a special advantage in homogeneous assays because fewer sample-preparation steps will be required. Finally, the fluorescer and quencher groups can be easily placed in internal or terminal positions in PNA. PNA is easily synthesized by standard peptide methods, and the required monomeric derivatives are readily prepared by simple reactions. We are exploring the development of fluorescer/quencher-linked PNA as probes for nucleic acids.

EXPERIMENTAL SECTION

General. DNA oligomers were purchased from Midland Certified Reagent Company, purified by gel filtration, and characterized by MALDI-TOF mass spectrometry. The extinction coefficients of DNA oligomers were calculated using the nearest-neighbor values: DNA(1), $\epsilon_{260} = 238\,200$ M^{-1} cm^{-1}; DNA(2), $\epsilon_{260} = 120\,200$ M^{-1} cm^{-1}. Similarly, PNA oligomers' extinction coefficients were determined using DNA values, with acridine or anthraquinone substituted for adenine: PNA(1)(1), $\epsilon_{260} = 233\,000$ M^{-1} cm^{-1}; PNA(2), $\epsilon_{260} = 227\,000$ M^{-1} cm^{-1}; PNA(3), $\epsilon_{260} = 232\,900$ M^{-1} cm^{-1}. The samples for all experiments were prepared in a 10 mM sodium phosphate buffer at pH 7.0. Spectra were recorded with the following instruments: Cary 1E (UV−vis), SPEX 1681 FLUOROLOG (Fluorescence), and Jasco J-270 (CD). Samples for induced circular dichroism spectroscopy (CD) were prepared in a 3 mL round cell with a 1 cm path length (Starna Cell Inc.). These spectra were recorded from 220 to 320 nm.

3,6-Diaza-(N³-2-anthraquinoyl)-N6-Boc-hexanoic acid (Monomer Q). Anthraquinone-2-carboxylic acid (2 g, 7.9 mmol), DCC (1.7 g, 8.3 mmol), *O*-(7-benzotriazole-1-yl)-1,1,3,3-tetramethyluronium-hexafluorophosphate (HOBT, 1.08 g, 8.0 mmol), and methyl(*N*-(2-Boc-aminoethyl))glycinate (2 g, 8.6 mmol) were dissolved in DMF (25 mL) and stirred at room temperature overnight. The reaction mixture was filtered, and the filtrate was washed with CH_2Cl_2 (2 × 25 mL). The solution was extracted with dilute $NaHCO_3$ (3 × 25 mL), 2 M $NaHSO_4$ (2 × 25 mL), and brine. The organic phase was dried with $MgSO_4$, filtered, and evaporated to dryness under reduced pressure. The yellow foam was dissolved in THF (10 mL), and 1 M LiOH (30 mL) was added. The mixture was stirred for 2 h. THF was removed from the solution under reduced pressure, and the pH was adjusted to 2.8 with 2 M $NaHSO_4$. The precipitate was extracted with CH_2Cl_2 (2 × 25 mL), evaporated to dryness, and then redissolved in ethyl acetate (3 mL). The ethyl acetate solution was poured into hexane (150 mL), and the precipitate that formed was collected. Yield: 3.1 g (87%). H^1-NMR DMSO-d_6 d: 7.81−8.30 (m, 7 H, aromatics); 6.98 and 7.72 (m, 1 H, BocNH); 4.17 and 3.97 (s, 2 H, CH_2O); 3.52 and 3.24 (m, 2 H, CH2); 3.21 and 3.02 (m, 2 H, CH_2); 1.17 and 1.19 (s, 9 H, Boc).

9-(5-Carboxypentyl)-aminoacridine. 6-Aminohexanoic acid (1.47 g, 11.2 mmol) was added to a solution of 9-phenoxyacridine (2.7 g, 10 mmol) in phenol (15 g). The suspension was stirred at 120 °C for 2 h. The solution was cooled to room temperature and poured into ether. The product precipitated as a yellow-green solid. It was triturated with hot ethanol, filtered, and then washed with ethanol, giving crude 9-(5-carboxypentyl)aminoacridine. Yield: 2.4 g (78%). H^1-NMR DMSO-d_6 d: 8.27 (d, 2 H, acr 2, 8); 7.61 (m, 4 H, acr 2, 3, 6, 7); 7.26 (m, 2 H, acr 4, 5); 3.79 (t, 2 H, CH_2CO); 2.16 (t, 2 H, CH_2N); 1.72, 1.50, and 1.37 (m, 2 H, CH_2). $C_{19}H_{20}N_2O_2$ calcd: 308. Found: 308.

3,10-Diaza-(N³-Boc-aminoethyl)-(N¹⁰-9-acridinyl)-4-oxodecanoic Acid (Monomer Ar). A mixture of 9-(5-carboxypentyl)aminoacridine (1 g, 3.2 mmol), diisopropylethylamine (0.9 g, 6.9 mmol), and *O*-(7-azabenzotriazole-1-yl)-1,1,3,3-tetramethyluronium-hexafluorophosphate (HATU, 1.34 g, 3.5 mmol) was stirred at room trremperature for 10 min in DMF (30 mL). Boc-aminoethylglycine (0.9 g, 3.8 mmol) was added, and the solution was stirred at 60 °C for 4 h. The solution was cooled, and CH_2Cl_2 (60 mL) was added. The reaction solution was extracted with 0.5 M $NaHCO_3$ (3 × 30 mL), 2 M $NaHSO_4$ (2 × 30 mL), and then brine. The organic phase was dried with $MgSO_4$ and evaporated to dryness. The residue was dissolved in THF/1 M LiOH (2:10) (40 mL), and the pH of the solution was adjusted to 2.8 with $NaHSO_4$ whereby an oil precipitated. The water phase

was decanted, and the oil was dissolved in ethanol (5 mL). The solution was poured into ether, and 3*N*-(Boc-aminoethyl)-10*N*-(9-acridinyl)-3,10-diaza-4-oxy-nonanic acid precipitated. Yield: 1.2 g (76%). H^1-NMR DMSO-d_6 d: 8.51 (d, 2 H, acr 2, 8); 7.90 (m, 2 H, acr 2, 7); 7.82 (m, 2 H, acr 3, 6); 7.71 (m, 1 H, NH); 6.83 and 6.45 (m, 1 H, BocNH); 7.51 (m, 2 H, acr 4, 5); 4.01 (m, 2 H, CH_2CO); 3.98 and 3.88 (s, 2 H, CH_2CO); 3.23, 3.00, 2.30, 2.03, and 1.88 (m, 2 H, CH_2); 2.16 (t, 2 H, CH_2N). $C_{27}H_{36}N_4O_5$ calcd: 508. Found: 508.

Synthesis of PNA Oligomers. The monomers described above were incorporated by the oligomerzation procedure previously described (*38*). However, the PNA syntheses containing the donor moieties constituted a special case because the capping step was omitted in the part of the synthesis including and following the donor monomer. However, to obtain high coupling yields, monomeric moieties of this part of the synthesis were double coupled. All oligomers were cleaved from the resin with trifluoromethanesulfonic acid and purified by HPLC. The identity of each oligomer was confirmed by mass spectroscopy. PNA(1): calcd m/e = 6492; found m/e = 6499. PNA(2): calcd m/e =6564; found m/e = 6563. PNA(3): calcd m/e = 6636; found m/e = 6631.

Formation of Stable PNA/DNA Hybrids: Thermal Denaturation Studies. Samples were prepared consisting of equimolar concentrations of PNA and DNA oligomers (1.0 or 2.0 μM each) in 1.0 mL of 10 mM sodium phosphate buffer (pH = 7.0). The PNA strand will often precipitate upon addition of the phosphate, presumably due to complexation of the lysine units by the phosphate. Mixing and addition of the DNA strand results in dissolution of the PNA. Samples were placed in cuvettes (1.5 mL capacity, 1.0 cm path length) and sealed with tape to prevent evaporation of water during heating/cooling cycles. The absorbance of the samples at 260 nm was monitored as a function of temperature for three consecutive runs: heating at 1.0 °C/min, cooling at 0.5 °C/min, and heating again at 0.5 °C/min.

The absorbance was plotted versus temperature for each sample. Melting temperatures (T_m) were determined as the maxima of plots of the first derivative of absorbance with respect to temperature, assuming a first-order phase transition. T_m values given in the text and tables have error values of ±0.5 °C.

REFERENCES

1. Nielsen, P. E., and Haaima, G. (1997) *Chem. Soc. Rev. 26*, 73−78.
2. Nielsen, P. E., Egholm, M., and Buchardt, O. (1994) *Bioconjugate Chem. 5*, 3−7.
3. Nielsen, P. E., Egholm, M., Berg, R. H., and Buchardt, O. (1991) *Science 254*, 1497−1500.
4. Egholm, M., Buchardt, O., Nielsen, P. E., and Berg, R. H. (1992) *J. Am. Chem. Soc. 114*, 1895−1897.
5. Egholm, M., Nielsen, P. E., Buchardt, O., and Berg, R. H. (1992) *J. Am. Chem. Soc. 114*, 9677−9678.
6. Brown, S. C., Thomson, S. A., Veal, J. M., and Davis, D. G. (1994) *Science 265*, 777−780.
7. Kastrup, J. S., Pilgaard, M., Jorgensen, F. S., Nielsen, P. E., and Rasmussen, H. (1995) *FEBS Lett. 363*, 115−117.
8. Erikkson, M., and Nielsen, P. E. (1996) *Nat. Struct. Biol. 3*, 410−413.
9. Jensen, K. K., Orum, H., Nielsen, P. E., and Norden, B. (1997) *Biochemistry 36*, 5072−5077.
10. Almarsson, O., Bruice, T. C., Kerr, J., and Zuckerman, R. N. (1993) *Proc. Natl. Acad. Sci. U.S.A. 90*, 7518−7522.
11. Cherny, D. Y., Belotserkovslii, B. P., Frank-Kamenetskii, M. D., Egholm, M., Buchardt, O., Berg, R. H., and Nielsen, P. E. (1993) *Proc. Natl. Acad. Sci. U.S.A. 90*, 1667−1670.
12. Peffer, N. J., Harvey, J. C., Bisi, J. E., Thomson, S. A., Hassman, C. F., Noble, S. A., and Babiss, L. E. (1993) *Proc. Natl. Acad. Sci. U.S.A. 90*, 10648−10652.
13. Griffith, M. C., Risen, L. M., Greig, M. J., Lesnik, E. A., Sprankle, K. G., Griffey, R. H., Kiely, J. S., and Freier, S. M. (1995) *J. Am. Chem. Soc. 117*, 831−832.
14. Wittung, P., Nielsen, P., and Norden, B. (1997) *J. Am. Chem. Soc. 119*, 3189−3190.
15. Hilbers, C. W., Haasnoot, C. A. G., de Bruin, S. H., Joordens, J. J. M., Van Der Marel, G. A., and Van Boom, J. H. (1985) *Biochimie 67*, 685−695.
16. Tyagi, S., and Kramer, F. R. (1996) *Nat. Biotechnol. 14*, 303−308.
17. Wang, J., Palacek, E., Nielsen, P. E., Rivas, G., Cai, X., Shiraishi, H., Dontha, N., Lou, D., and Farias, P. A. M. (1996) *J. Am. Chem. Soc. 118*, 7667−7670.
18. Wang, J., Rivas, G., Cai, X., Chicharro, M., Parrado, C., Dontha, N., Begleiter, A., Mowat, M., Palacek, E., and Nielsen, P. E. (1997) *Anal. Chim. Acta 344*, 111−118.
19. Schefeler, I. E., Elson, E. L., and Baldwin, R. L. (1968) *J. Mol. Biol. 36*, 291−304.
20. Haasnoot, C. A. G., De Bruin, S. H., Berendsen, R. G., Janssen, H. G. J. M., Binnendijk, T. J. J., Hilbers, C. W., van der Marel, G. A., and van Boom, J. H. (1983) *J. Biomol. Struct. Dyn. 1*, 115−129.
21. Tomac, S., Sarkar, M., Ratilainen, T., Wittung, P., Nielsen, P. E., Nordén, B., and Gräslund, A. (1996) *J. Am. Chem. Soc. 118*, 5544−5552.
22. Armitage, B., Ly, D., Koch, T., Frydenlund, H., Orum, H., and Schuster, G. B. (1997) *Proc. Natl. Acad. Sci. U.S.A. 94*, 12320−12325.
23. Egholm, M., Buchardt, O., Christensen, L., Behrens, C., Freier, S. M., Driver, D. A., Berg, R. H., Kim, S. K., Nordén, B., and Nielsen, P. E. (1993) *Nature 365*, 566−568.
24. Kim, S. K., Nielsen, P. E., Egholm, M., Buchardt, O., Berg, R. H., and Norden, B. (1993) *J. Am. Chem. Soc. 115*, 6477−6481.
25. Wittung, P., Nielsen, P. E., Buchardt, O., Egholm, M., and Norden, B. (1994) *Nature 368*, 561−563.
26. Wittung, P., Eriksson, M., Lyng, R., Nielsen, P. E., and Norden, B. (1995) *J. Am. Chem. Soc. 117*, 10167−10173.
27. Wakelin, L. P. G., Romanos, M., Chen, T. K., Glaubiger, D., Canellakis, E. S., and Waring, M. J. (1978) *Biochemistry 17*, 5057−5063.
28. Kubota, Y., and Motoda, Y. (1980) *J. Phys. Chem. 84*, 2855−2861.
29. Li, F. N., Rodin, O. G., Redchenko, V. V., and Traven, V. F. (1991) *Zh. Obshch. Khim. 61*, 186−191.
30. Shen, T., Zhao, Z.-G., and Xu, H.-J. (1992) *Sci. China, Ser. B 35*, 137−145.
31. Breslin, D. T., and Schuster, G. B. (1996) *J. Am. Chem. Soc. 118*, 2311−2319.
32. Rehm, D., and Weller, A. (1970) *Isr. J. Chem. 8*, 259.
33. Beratan, D. N., Priyadarshy, S., and Risser, S. M. (1997) *Chem. Biol. 4*, 3−8.
34. Arkin, M. R., Stemp, E. D., Pulver, S. C., and Barton, J. K. (1997) *Chem. Biol. 4*, 389−400.
35. Dandliker, P. J., Holmlin, R. E., and Barton, J. K. (1997) *Science 275*, 1465−1468.
36. Hall, D. B., Holmlin, R. E., and Barton, J. K. (1996) *Nature 382*, 731−735.
37. Meade, T. J., and Kayyem, J. F. (1995) *Angew. Chem., Int. Ed. Engl. 34*, 352−354.
38. Nielsen, P., Egholm, M., Buchardt, O., Sonnechesen, S., Lohse, J., Manoharan, M., Kiely, J., Griffith, M., and Sprankle, K. (1995) World Intellectual Property Organization, October 6, 1995.

BI9729458